Entanglement induced by nonadiabatic chaos

Hiroshi Fujisaki*
Department of Chemistry, Boston University, Boston, Massachusetts, 02215, USA
(Received 6 January 2004; revised manuscript received 25 February 2004; published 29 July 2004)

We investigate entanglement between electronic and nuclear degrees of freedom for a model nonadiabatic system. We find that entanglement (measured by the von Neumann entropy of the subsystem for the eigenstates) becomes nearly maximum when the system shows "nonadiabatic chaos" behavior which was found in our previous work [Phys. Rev. E **63**, 066221 (2001)], but the reverse is not necessarily the case.

DOI: 10.1103/PhysRevA.70.012313 PACS number(s): 03.67.−a, 33.80.Be, 05.45.Mt, 03.65.Ud

I. INTRODUCTION

Quantum information processing (QIP) is one of the hot topics in many branches of science [1]. One important point is how to implement a quantum computer in real systems, and many possibilities have been theoretically suggested and experimentally tested. One candidate can be molecular systems because highly excited molecules have dense quantum states, which can be manipulated by laser fields. Some quantum logic gates in such a system can be built by using optimal control theory [2], and are actually realized in a molecular system [3].

In highly excited molecules or laser-driven molecular systems, nonadiabatic transition (NT) is a rule rather than an exception [4,5], i.e., we have to consider both electronic and nuclear degrees of freedom (DOF) at the same time without invoking the Born-Oppenheimer approximation. In such a case, a fundamental issue related to QIP is how much (quantum) entanglement is produced between electronic and nuclear DOF in molecular systems, because entanglement is a key ingredient in QIP.

Here we investigate a two-mode–two-state (TMTS) system which has two electronic DOF and two nuclear (vibrational) DOF with a nonadiabatic coupling [6,7]. This is a (minimum) model NT system which shows "quantum chaos" behavior, i.e., statistical properties of energy levels and eigenstates are similar to those of a random matrix system [8]. If many electronic DOF are involved, the similar system has a naive classical limit, and its dynamical property of entanglement has been already addressed in Ref. [9]. In such a case, a quantum chaological view is effective, and we can say much about a quantum system by studying its classical limit [9]: Furuya *et al.* treated a nine-atom Jayes-Cummings model (where nine spin-1/2's are coupled to one vibrational mode) because the model has a semiclassical regime. However, the situation is different and more difficult here, because the TMTS system does not have a naive classical limit due to discreteness of the electronic DOF: the TMTS system (where one spin-1/2 is coupled to two vibrational modes) is not expected to have such a semiclassical regime as mentioned in Ref. [9]. Since we cannot adapt a naive quantum-classical correspondence to analyze the result [10], the entanglement production in the TMTS system is a challenging problem and deserves further attention.

II. TMTS SYSTEM

The TMTS system in the diabatic representation is described by the following Hamiltonian:

$$\mathcal{H}_{\mathrm{TMTS}} = \begin{pmatrix} T_{\mathrm{kin}} + V_A & J \\ J & T_{\mathrm{kin}} + V_B \end{pmatrix}, \tag{1}$$

where T_{kin} is the kinetic energy, $V_i (i=A,B)$ is the potential energy for state i defined by

$$T_{\mathrm{kin}} = \tfrac{1}{2}(p_x^2 + p_y^2), \tag{2}$$

$$V_i = \tfrac{1}{2}(\omega_x^2 \xi_i^2 + \omega_y^2 \eta_i^2) + \epsilon_i \quad (i = A,B) \tag{3}$$

with

$$\xi_A = x \cos\theta - (y-a)\sin\theta, \tag{4}$$

$$\eta_A = x \sin\theta + (y-a)\cos\theta, \tag{5}$$

$$\xi_B = x \cos\theta + (y+a)\sin\theta, \tag{6}$$

$$\eta_B = -x \sin\theta + (y+a)\cos\theta. \tag{7}$$

The geometrical meaning of the parameters is shown in Fig. 1. Note that we have just used a harmonic potential for each electronic state.

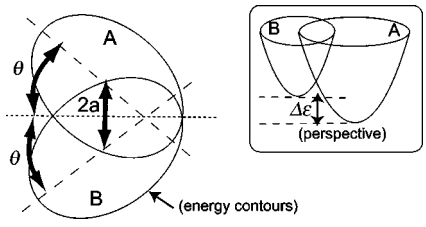

FIG. 1. A schematic representation of the TMTS system. The distance between the minima of the potential is $2a$, and the angle between the relevant crossing seam (dotted line) and the primary axis of each potential (dashed line) is θ. Inset, the perspective of the TMTS system. The potential minima are different with $\Delta\epsilon = \epsilon_B - \epsilon_A = 0.173$.

*Electronic address: fujisaki@bu.edu

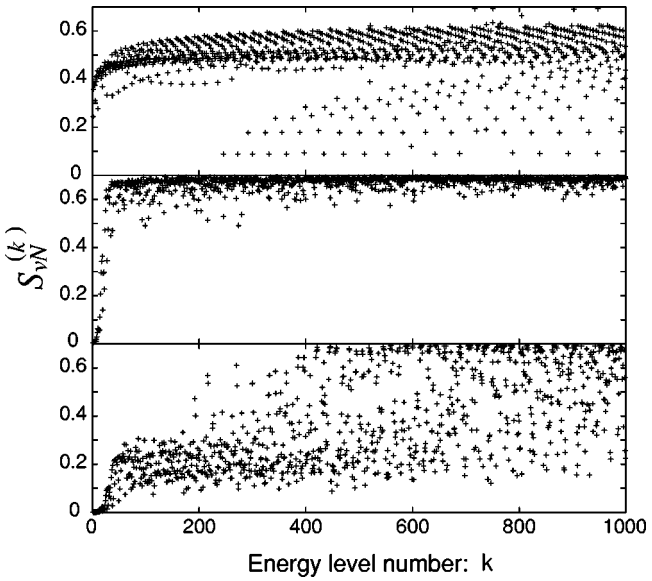

FIG. 2. J dependence of entanglement production measured by the von Neumann entropy as a function of the energy level number. Top, $J=7.5$. Middle, $J=1.5$. Bottom, $J=0.3$. The Duschinsky angle is fixed as $\theta=\pi/6$.

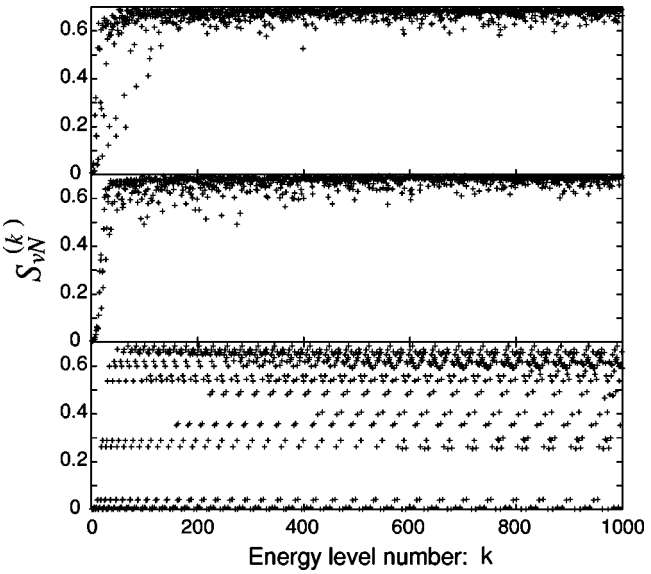

FIG. 3. θ dependence of entanglement production measured by the von Neumann entropy as a function of the energy level number. Top, $\theta=\pi/3$. Middle, $\theta=\pi/6$. Bottom, $\theta=0.0$. The nonadiabatic coupling is fixed as $J=1.5$.

Here the Duschinsky angle θ [11] and the nonadiabatic coupling constant J are two important parameters for the system; the latter induces entanglement between electronic and vibrational DOF. We solve this Hamiltonian according to the procedure in Ref. [6], and obtain the eigenenergies and eigenvectors. The kth eigenvector can be written as

$$|\Phi^{(k)}\rangle = \sum_{i=1}^{2}\sum_{j} C_{ij}^{(k)}|i\rangle\rangle|j\rangle = \sum_{i=1}^{2}|\phi_i^{(k)}\rangle|i\rangle\rangle, \tag{8}$$

where $|1\rangle\rangle=(|A\rangle+|B\rangle)/\sqrt{2}$, $|2\rangle\rangle=(-|A\rangle+|B\rangle)/\sqrt{2}$, $|A\rangle$, $|B\rangle$ are the electronic bases for diabatic surfaces A and B, respectively, $|j\rangle$ represents two-dimensional harmonic eigenfunctions, and $|\phi_i^{(k)}\rangle\equiv\langle\langle i|\Phi^{(k)}\rangle=\Sigma_j C_{ij}^{(k)}|j\rangle$.

From this eigenvector, we can construct a reduced density operator for the electronic DOF as

$$\rho^{(k)} = \mathrm{Tr}_{\mathrm{vib}}\{|\Phi^{(k)}\rangle\langle\Phi^{(k)}|\} = \begin{pmatrix}\rho_{11}^{(k)} & \rho_{12}^{(k)}\\ \rho_{21}^{(k)} & \rho_{22}^{(k)}\end{pmatrix} = \begin{pmatrix}\sum_j C_{1,j}^{(k)}(C_{1,j}^{(k)})^* & \sum_j C_{1,j}^{(k)}(C_{2,j}^{(k)})^*\\ \sum_j C_{2,j}^{(k)}(C_{1,j}^{(k)})^* & \sum_j C_{2,j}^{(k)}(C_{2,j}^{(k)})^*\end{pmatrix}, \tag{9}$$

where $C_{i,j}^{(k)}$ are actually all real numbers.

The measure of entanglement we choose here is the von Neumann entropy of the subsystem defined by

$$S_{\mathrm{vN}}^{(k)} = -\mathrm{Tr}\{\rho^{(k)}\ln\rho^{(k)}\} = -\lambda_1^{(k)}\ln\lambda_1^{(k)} - \lambda_2^{(k)}\ln\lambda_2^{(k)}, \tag{10}$$

where $\lambda_i^{(k)}$ $(i=1,2)$ is an eigenvalue for the 2×2 matrix, Eq. (9). A note is in order: the value of the entropy is the same if we use the reduced density operator for the vibrational DOF. We took the electronic DOF because the 2×2 matrix is very easy to diagonalize, and to interpret the result as shown below.

III. NUMERICAL RESULTS

First we show the J dependence of the results fixing $\theta=\pi/6$: As we can see in Fig. 2, the entropies for the case of $J=1.5$ assemble around its maximum $S_{\mathrm{vN}}\simeq\log 2$, whereas those of the other cases $(J=0.3,7.5)$ are rather broadly distributed. This condition of entanglement is very similar to that of quantum chaos behavior found in Ref. [6]: When both J and θ have "intermediate" values ($J\simeq1$ and $\theta\simeq\pi/4$), the system shows the quantum chaos behavior, i.e., the nearest neighbor spacing distribution becomes the Wigner type, Δ_3 statistics become a log curve, and the amplitude distribution of the eigenstates becomes Gaussian. To further confirm this, we show the θ dependence of the results fixing $J=1.5$ in Fig. 3. This result also nicely corresponds to the previous condition for the quantum chaos behavior. From these results, we can conclude that *when the TMTS system shows the quantum chaos behavior, the entanglement between the electronic and vibrational DOF becomes nearly maximum*.

However, as noticed in Figs. 2 and 3, the amount of entanglement strongly varies depending on *each* eigenstate for the cases of $J=0.3$ and 7.5 or $J=1.5$ with $\theta=0$. To consider this problem, we rewrite the entropy (entanglement) using the vibrational bases for each electronic state, $|\phi_A^{(k)}\rangle$ and $|\phi_B^{(k)}\rangle$. These states are connected to the above states $|\phi_1^{(k)}\rangle$ and $|\phi_2^{(k)}\rangle$ by

$$|\phi_A^{(k)}\rangle = \frac{1}{\sqrt{2}}(|\phi_1^{(k)}\rangle - |\phi_2^{(k)}\rangle), \tag{11}$$

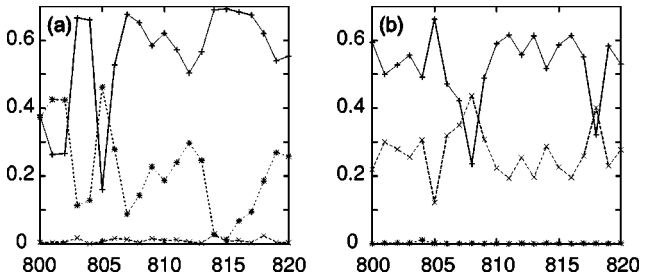

FIG. 4. $S_{\mathrm{vN}}^{(k)}(+)$, $|\Delta P_{AB}^{(k)}|(*)$, and $|S_{AB}^{(k)}|(\times)$ as a function of energy level number. (a) $J=0.3$ (weakly nonadiabatic case). (b) $J=7.5$ (strongly nonadiabatic case). (Lines are just for guiding eyes.) The Duschinsky angle is fixed as $\theta=\pi/6$.

$$|\phi_B^{(k)}\rangle = \frac{1}{\sqrt{2}}(|\phi_1^{(k)}\rangle - |\phi_2^{(k)}\rangle). \tag{12}$$

Hence the density operator, Eq. (9), is represented as

$$\rho_{11}^{(k)} = \tfrac{1}{2} + \langle\phi_A^{(k)}|\phi_B^{(k)}\rangle \equiv \tfrac{1}{2} + S_{AB}^{(k)}, \tag{13}$$

$$\rho_{22}^{(k)} = \tfrac{1}{2} - \langle\phi_A^{(k)}|\phi_B^{(k)}\rangle \equiv \tfrac{1}{2} - S_{AB}^{(k)}, \tag{14}$$

$$\rho_{12}^{(k)} = \tfrac{1}{2}(\langle\phi_A^{(k)}|\phi_A^{(k)}\rangle - \langle\phi_B^{(k)}|\phi_B^{(k)}\rangle) \equiv \Delta P_{AB}^{(k)}, \tag{15}$$

where we have introduced two new parameters: $S_{AB}^{(k)}$ is the overlap between the kth eigenstates on surfaces A and B, and $\Delta P_{AB}^{(k)}$ is the half of the population difference between the kth eigenstates on surfaces A and B. Using these parameters, the eigenvalues for the entropy are written as

$$\lambda_{1,2}^{(k)} = \tfrac{1}{2} \pm \sqrt{|S_{AB}^{(k)}|^2 + |\Delta P_{AB}^{(k)}|^2}. \tag{16}$$

From this relation, for the entropy to be large, *both* $|S_{AB}^{(k)}|$ and $|\Delta P_{AB}^{(k)}|$ should be small. We can numerically confirm this property for the strongly "chaotic" case ($J=1.5$), which is a natural consequence of that $|\phi_{A,B}^{(k)}\rangle$ are random vectors. For less "chaotic" cases ($J=0.3, 7.5$), the situation is different: As shown in Fig. 4, there is a strong correlation between $S_{\mathrm{vN}}^{(k)}$ and $|\Delta P_{AB}^{(k)}|$ for the weakly nonadiabatic case ($J=0.3$), whereas between $S_{\mathrm{vN}}^{(k)}$ and $|S_{AB}^{(k)}|$ for the strongly nonadiabatic case ($J=7.5$). On the other hand, $|S_{AB}^{(k)}| \simeq 0$ for the former and $|\Delta P_{AB}^{(k)}| \simeq 0$ for the latter. This is interpreted as follows: For the former, the eigenstates "reside" on diabatic surfaces A and B which are tilted. Thus the overlapping between the eigenstates $|S_{AB}^{(k)}|$ becomes small because the nodal patterns for the eigenstates are also tilted (see Fig. 5 in Ref. [6]). For the latter, the eigenstates "reside" on adiabatic surfaces, and the amplitudes of them on diabatic surfaces A and B are similar (see Fig. 7 in Ref. [6]), hence $|\Delta P_{AB}^{(k)}| \simeq 0$.

Let us focus on the weakly nonadiabatic case ($J=0.3$). In the range of $k=800$ to 820, the lowest entangled state is 805th ($S_{\mathrm{vN}}^{(805)} \simeq 0.15$), and the highest is 815th ($S_{\mathrm{vN}}^{(815)} \simeq \log 2$) [Fig. 4(a)]. In Figs. 5 and 6, we show the two eigenstates on diabatic surfaces A and B. As anticipated from the above argument, there is a large population difference on surfaces A and B for the less entangled state, whereas there is not for the strongly entangled state. The latter situation

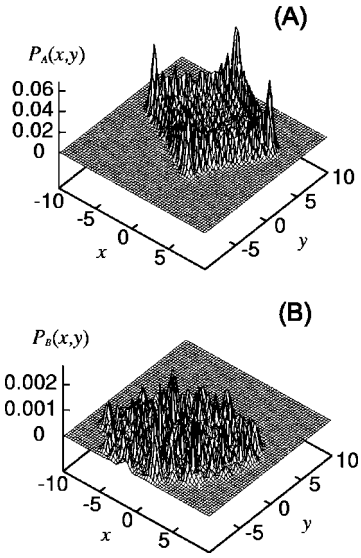

FIG. 5. A less entangled regular state: 805 eigenstates on diabatic surfaces A (A) and B (B) for the weakly nonadiabatic case: $J=0.3$. $P_i(x,y)=|\langle x,y|\phi_i\rangle|^2$ ($i=A,B$). Note that the scale for (B) is smaller than that for (A). The Duschinsky angle is fixed as $\theta=\pi/6$.

means that even a regular state can strongly entangle. Note that, albeit we desymmetrized the system with a finite $\Delta\epsilon=\epsilon_A-\epsilon_B$, we have this entangled state for the regular case. If we do not desymmetrize the system, i.e., $\Delta\epsilon=0$, we easily have entangled states for both regular and chaotic cases because of the symmetry of the system.

Thus we must be cautious to use the entanglement production as a manifestation of quantum chaotic behavior [9,12]: when the TMTS system shows the quantum chaos

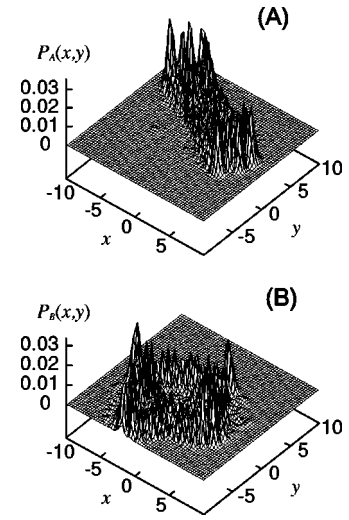

FIG. 6. A strongly entangled regular state: 815 eigenstates on diabatic surfaces A (A) and B (B) for the weakly nonadiabatic case: $J=0.3$. $P_i(x,y)=|\langle x,y|\phi_i\rangle|^2 (i=A,B)$. The Duschinsky angle is fixed as $\theta=\pi/6$.

behavior, the entanglement becomes nearly maximum (log 2), however, the reverse is not true: nearly maximum entanglement can arise even in the regular cases as shown above. That is, the correspondence between the entanglement production and quantum chaos behavior in the TMTS system is not one-to-one. This result has an important implication for the dynamical behavior of entanglement [9,12,13]. If we can prepare a nearly nonentangled wave packet consisting of entangled eigenstates for the "regular" case (as a simple example of a two spin-1/2 system, consider the case $|\uparrow\downarrow\rangle \propto (|\uparrow\downarrow\rangle+|\downarrow\uparrow\rangle)+(|\uparrow\downarrow\rangle-|\downarrow\uparrow\rangle)$), this state can produce entanglement in time, and the temporal amount of entanglement might be comparative to that of the "chaotic" case. This issue will be pursued elsewhere.

IV. SUMMARY

In this paper, we investigated quantum entanglement production between electronic and nuclear (vibrational) degrees of freedom for a two-mode–two-state (TMTS) system. We found that the entanglement in the eigenstates becomes nearly maximum when the TMTS system shows the quantum chaos behavior, i.e., its statistical properties are similar to those of a random matrix system. However, we also showed that the regular regions of the TMTS system can cause nearly maximum entanglement. It thus should be cautious to use entanglement production as a manifestation of the quantum chaos behavior. It will be interesting to analyze other nonadiabatic systems like Jahn-Teller molecules [14] in light of entanglement production.

[1] M. A. Nielsen and I. L. Chuang, *Quantum Computation and Quantum Information* (Cambridge University Press, Cambridge, 2000).

[2] J. P. Palao and R. Kosloff, Phys. Rev. Lett. **89**, 188301 (2002); Phys. Rev. A **68**, 062308 (2003).

[3] J. Vala, Z. Amitay, B. Zhang, S. R. Leone, and R. Kosloff, Phys. Rev. A **66**, 062316 (2002).

[4] H. Nakamura, *Nonadiabatic Transition: Concepts, Basic Theories and Applications* (World Scientific, Singapore, 2002); C. Zhu, Y. Teranishi, and H. Nakamura, Adv. Chem. Phys. **117**, 127 (2001).

[5] K. Takatsuka, Y. Arasaki, K. Wang, and V. McKoy, Faraday Discuss. **115**, 1 (2000); Y. Arasaki, K. Takatsuka, K. Wang, and V. McKoy, Phys. Rev. Lett. **90**, 248303 (2003).

[6] H. Fujisaki and K. Takatsuka, Phys. Rev. E **63**, 066221 (2001); see also J. Chem. Phys. **114**, 3497 (2001); H. Higuchi and K. Takatsuka, Phys. Rev. E **66**, 035203(R) (2002).

[7] E. J. Heller, J. Chem. Phys. **92**, 1718 (1990).

[8] M. C. Gutzwiller, *Chaos in Classical and Quantum Mechanics* (Springer-Verlag, New York, 1990).

[9] K. Furuya, M. C. Nemes, and G. Q. Pellegrino, Phys. Rev. Lett. **80**, 5524 (1998).

[10] Note, on the other hand, that there is a sound correspondence between the TMTS system and its mapping (quasiclassical) system. See H. Fujisaki, Phys. Rev. E **69**, 037201 (2004).

[11] See J. Tang, M. T. Lee, and S. H. Lin, J. Chem. Phys. **119**, 7188 (2003), and references therein.

[12] X. Wang, S. Ghose, B. C. Sanders, and B. Hu, e-print quant-ph/0312047.

[13] A. Tanaka, H. Fujisaki, and T. Miyadera, Phys. Rev. E **66**, 045201(R) (2002); H. Fujisaki, T. Miyadera, and A. Tanaka, *ibid.* **67**, 066201 (2003); H. Fujisaki, A. Tanaka, and T. Miyadera, J. Phys. Soc. Jpn. **72**, 111 (2003); e-print quant-ph/0302015.

[14] H. Köppel, W. Domcke, and L. S. Cederbaum, Adv. Chem. Phys. **57**, 59 (1984); D. M. Leitner, H. Köppel, and L. S. Cederbaum, J. Chem. Phys. **104**, 434 (1996); H. Yamasaki, Y. Natsume, A. Terai, and K. Nakamura, Phys. Rev. E **68**, 046201 (2003); A. P. Hines, C. M. Dawson, R. H. McKenzie, and G. J. Milburn, e-print quant-ph/0402016.